A Final Report to

The National Aeronautics and Space Administration

Grant NAGW-1767

Application of Lightning Data to Satellite-Based Rainfall Estimation

For the Period of

1 January 1989 through 31 December 1991

Submitted by

David W. Martin, Principal Investigator

Barry B. Hinton, Co-Investigator

Brian A. Auvine

Space Science and Engineering Center

at the University of Wisconsin-Madison

1225 West Dayton Street

Madison, Wisconsin 53706

(608) 262 0544

15 October 1991

TABLE OF CONTENTS

ABSTRACT

Information on lightning may improve rain estimates made from infrared images of a geostationary satellite. We address this proposition through a case from the Cooperative Huntsville Meteorological Experiment (COHMEX). During the afternoon and evening of 13 July 1986 waves of showers and thunderstorms developed over and near the lower Tennessee River valley. For the shower and thunderstorm region within 200 km of the National Weather Service radar at Nashville, Tennessee, we measure cold-cloud area in a sequence of GOES infrared images covering all but the end of the shower and thunderstorm period. From observations of the NASA/Marshall direction-finding network in this small domain, we also count cloud-to-ground lightning flashes and, from scans of the Nashville radar, we calculate volume rain flux. Using a modified version of the Williams and Houze scheme, over an area within roughly 240 km of the radar (the "large domain"), we identify and track cold cloud systems. For these systems, over the large domain we measure area and count flashes; over the small domain, we calculate volume rain flux.

For a temperature threshold of 235K, peak cloud area over the small domain lags both peak rain flux and peak flash count by about four hours. At a threshold of 226K the lag is about two hours. Flashes and flux are matched in phase. Over the large domain nine storm systems occur. These range in size from 300 to 60,000 km^2; in lifetime, from about 2 1/2 h to 6 h or more. Storm system area lags volume rain flux and flash count; nevertheless it is linked with these variables. In essential respects the associations were the same when clouds were defined by a threshold of 226K. Tentatively, we conclude that flash counts complement infrared images in providing significant additional information on rain flux.

ACKNOWLEDGEMENTS

The data used in this study were provided by Steven J. Goodman. Dennis Buechler provided the software for rain flux calculations. Theresa Hart facilitated the transfer of data from MSFC to UW-Madison. David Santek assisted in the remapping of radar images.

A. INTRODUCTION

Since the launch of the first operational geostationary satellite in 1974, meteorologists have tested nearly a dozen techniques for the use of infrared image data to monitor rainfall (e.g., see Atlas and Thiele 1981; D'Souza and Barrett 1988; Martin et al. 1990). We believe it is fair to say that none of these techniques has lived up to the expectations of its author or authors. The principal reason for shortfalls among the infrared techniques is cirrus cloud. As Negri and Adler (1981) and Goodman et al. (1988) point out (also see Barrett and Martin 1981, pp 39 and 103-105), cirrus forms a canopy, through which the structures producing rain are dimly seen or totally obscured. Some imaging radiometers at frequencies outside the thermal infrared window can perceive more of this structure (Heymsfield and Fulton 1988), but typically their observations undersample convective rain.

As this limitation of satellite infrared images was being explored, studies of lightning advanced on three fronts. First, corporations, universities and agencies of government established operational and research networks for the detection of cloud-to-ground lightning flashes in the United States (Krider et al. 1980; Orville et al. 1983; Lyons et al. 1989; Goodman 1990). Second, where they overlapped rain gauges or the scans of weather radars, these networks yielded evidence of a coupling between lightning and convective rainfall (Grosh 1978; Piepgrass et al. 1982; Goodman et al. 1988; Goodman and Christian 1992; also see Cherna et al. 1985 and the references therein). Third, partly by design and partly by chance scientists discovered possibilities for observing lightning from space (Orville and Spencer, 1979). The conjunction of these advances recently led NASA to plan lightning sensors for a Geostationary Operational Environmental Satellite (GOES; Christian et al. 1989).

Our primary objective in this study is to test the proposition that information on cloud-to-ground lightning can improve rain estimates made from infrared images of a geostationary satellite. A secondary objective is to document the relationship between cloud, lightning and rainfall. In pursuing these objectives we anticipate the deployment of a lightning detector on a geostationary satellite by the end of the century.

B. METHOD

Given a series of infrared images, we wish to identify and isolate the more significant rain systems. By means of some simple algorithm, we estimate volume rain flux (hereafter, flux) for each system. From coincident ground observations of a direction-finding network, for each system we count flashes of cloud-to-ground lightning. The satellite estimate of flux is compared with a radar measurement. Differences between these two curves are, in turn, compared with flash counts.

As a baseline for the rain system results, we also estimate and measure flux and count flashes for the area of the radar scan. The scan-area results are equivalent to the rain system results only in the case of a single system entirely contained by the radar scan.

We expect at best a modest agreement between satellite and radar rain fluxes (e.g., see Lovejoy and Austin 1979; Richards and Arkin 1981; Barrett and Martin 1981; Griffith, 1987; Negri and Adler 1987). Satellite estimates tend to overestimate rain areas and underestimate peak rates. On convective time scales estimates based on infrared data, especially, tend to lag actual rain flux. The lag is largest for the warmer thresholds, which are most likely to include all significant rain systems.

Cirrus clouds complicate the tracking of individual rain systems (Stout et al. 1979; Negri et al. 1984; Goodman et al. 1988). For the present study we adapted the algorithm of Williams and Houze (1987) to the Man-computer Interactive Data Access System (McIDAS; Suomi et al. 1983). Like some others the Williams and Houze tracking algorithm employs a threshold of temperature to isolate candidate clouds. It also links a cloud or clouds in one image to a cloud or clouds in the next image of a sequence if there is some critical degree of overlap. The Williams and Houze algorithm differs from most others in allowing a link for overlap measured either forward or backward in time. The effect is to increase temporal continuity.

McIDAS has capabilities for digital enhancement of images and color superposition of paired images. Exploiting these capabilities and adapting the Williams and Houze algorithm, we developed a procedure for tracking clouds. The procedure employs duplicate sequences of infrared images. These are loaded as pairs, with one sequence--call it background--advanced by a single image with respect to the other (foreground) sequence (i.e., foreground image t1 is matched with background image t2). Color enhancements are applied to both image sequences such that all pixels lower than a certain digital count become black. Pixels higher than this threshold count are colored. The choice of colors is arbitrary, so long as the colors for each track are different. Apart from black, a superposed image, then, can have up to three colors. Each color is unique to a condition of the superposed image.

We define three types of cloud. In a foreground image an isolated cold feature is simply a *cloud*. Each member of a pair of coupled cold features also is considered to be a cloud up to a certain ratio of shared boundary to shared plus unshared boundary. This is a departure from the Williams and Houze algorithm. A cloud which shares area with one or more cold features in the matching background image is an *overlapping cloud*. The overlapping cloud is a *storm* if the overlap area exceeds a certain threshold value and if the overlap area is half or more of either foreground or background cloud area. If the storm is coupled by proximity to a

storm or overlapping clouds or clouds in the following overlap image, it becomes a *storm system.* These terms are explained more fully in Appendix A.

The sequence of pictures in Fig. 1 simulates the overlap procedure and illustrates the three types of cloud. The first picture (Fig. 1a) is an infrared image. The second (Fig. 1b) is a binary, digital enhancement of Fig. 1a; consider this to be the foreground image. The third picture (Fig. 1c) is an enhancement of the infrared image from one hour later; consider this to be the background image. The fourth picture (Fig. 1d) shows what happens when the second and third pictures are superposed. Clouds only (no overlap) are found in a cluster at the bottom of the picture. There also is an isolated cloud in the upper-right corner. A pair of overlapping clouds (which fail the storm overlap-area test) is found just to the right of center. In the upper-left quadrant is a storm.

Using a cursor-draw capability of McIDAS, we outline each foreground-image cloud which qualifies as an overlapping cloud or as a storm or which subsequently becomes a storm. Each outline hugs its cloud boundary. (Typically, the outline lies within 4 km of the cloud; never is it allowed to stray more than 10 km from the cloud.) The outline for the storm noted above is shown in the last picture of the sequence (Fig. 1e). Had either of the two overlapping clouds subsequently become a storm, they also would have been outlined.

Still using McIDAS, for each outline we count cold pixels, positive flashes and total flashes and we count reflective pixels as a function of reflectivity. Flashes are counted over a period defined by the "advanced" midpoints of the intervals on either side of the image in question; the advance (of four minutes) allows for the time between the first scan of the satellite (which determines the nominal image time) and the scans across the radar. Reflective pixels are counted for each radar image falling within a satellite image period. By means of a navigation transform we convert the number of cold pixels to a cloud area. This cloud area becomes a proxy for satellite (volume) rain flux (see Appendix B). By means of the relationship of Jones, as described by Goodman et al. (1988), and the same navigation transform, we convert reflectivity to radar (volume) rain flux.

C. DATA

In the meteorological record there are relatively few cases of storms scanned by geostationary satellite and by calibrated rain radar and at the same time monitored for lightning. The Cooperative Huntsville Meteorological Experiment (COHMEX; Dodge et al. 1986, also see Williams et al. 1987) may constitute the richest sample to date. COHMEX ran in June and July of 1986. It was headquartered in Huntsville, Alabama, and centered on Tennessee. Considering the availability of radar and lightning data, as well as coverage, we chose to study the case from COHMEX which began in the afternoon of 13 July 1986 and continued into the early morning of the following day. In a somewhat different context this case also has been studied by Goodman (1990).

The infrared images are from the GOES-East satellite. They cover the period from 1401 UTC on 13 July through 0500 UTC on the following day. (Hereafter, all times in this report are UTC.) Nominally, the interval is one hour. However, because of missing images or bad data, the intervals are as large as 90 minutes and as small as 30 minutes. There are 16 images in the sequence.

The navigation (image to earth coordinate transform) was adjusted by means of matching 2 km resolution visible images in which Gulf of Mexico barrier islands could be identified. Then infrared images were visually shifted in line and element to match corresponding visible images. Finally, by means of background thermal patterns corresponding to surface features such as coastlines, rivers and ridgelines we checked the full infrared sequence for image-to-image registration. Location uncertainty is greatest late in the renavigated sequence. However, we believe at all times it is less than 4 km.

We employed two threshold temperatures, 235K and 226K. (For the thermal infrared channel of the GOES 6 Visible and Infrared Spin Scan Radiometer, a digital count of 183 corresponds to a temperature of 235K; 192, to 226K.) Two-hundred thirty-five is the temperature which defines cold cloud in the GOES Precipitation Index (GPI; Arkin and Meisner, 1987). It is close to the temperature (238K) which Cherna et al (1985) selected as the GOES infrared threshold for summertime thunderstorms near Montreal. In the central Plains states and in the Tennessee River valley 226K is a critical temperature for a high probability of summertime lightning (Auvine and Martin, figure 5, 1987). Neither threshold is as cold as that used by McAnelly and Cotton (1989) to define mesoscale convective complexes over the central United States.

Rainfall data were extracted from base scans of the Nashville radar, which is located at $36^{0}15'$ N, $86^{0}34'$ W. During COHMEX this radar was equipped with a Radar Data Processor. Nominally, the radar completed a scan sequence every ten minutes. However, for this case ten-minute base scans are available only for part of the infrared sequence (1640 through 2340 and 0240 through 0350). Before 1640 and after 0350 no scans are available; between 2340 and 0240 only three are available. Scans were remapped to the projection of the GOES; all were used to calculate rainfall. We limit our rain flux analysis to the annulus between 20 and 200 km, centered on the radar. Errors are largest toward the circumference of the annulus, where the beam (of 2.2^{0} width) is about 4 km above the surface. There, in spite of the convective nature of the rain, the radar measurement is likely to be low (Joss and Waldvogel, 1990). We estimate the absolute error in a measurement of rain flux for a typical storm may be as much as 50%. Relative errors are significantly smaller.

Flashes were recorded and located by NASA's Lightning Location and Protection network. This is a direction-finding system. Nominally, it responds only to the cloud-to-ground flashes. We estimate that over the area of interest 80% or more of these are detected. Positive flashes are distinguished from negative flashes. For a more complete description of the system, see Williams et al. (1987) or Goodman et al (1988). Goodman (1990) describes the technique used to remove bias in calculations of the locations of flashes. Residual errors probably are not larger than twice the error in infrared pixel location; on average they are likely to be no larger than pixel location error.

Because convection in this case is confined to the southern half of the COHMEX area, effectively the 20/200 km annulus is truncated at the Tennessee-Kentucky border. The term "small domain" refers specifically to this truncated annulus (Fig. 2). Cloud and lightning analyses are allowed over the region defined by the 240 km range circle and the Tennesee-Kentucky border. This is the "large domain".

D. RESULTS

The infrared sequence, together with matching (daytime) visible images, shows convection developing in waves. Cumulus clouds appear first over Tennessee. At 1601 they comprise a band from north-central Tennessee across northern Alabama and into Mississipi. By 1631 the band contains congestus clouds; by 1701, small cumulonimbus clouds. Thereafter, until 0500 cumulonimbus clouds in every stage of development are present nearly continuously over Tennessee and the states to the south.

1. Threshold 235K

We first present the results for threshold 235K. These, in turn, are given first for the small domain, then for the large domain.

a. Small Domain

This part of the analysis is keyed to a fixed area. Cloud area (Fig. 3a) shows a single peak 6 to 7 h after the appearance of cold cloud. Two inflections to the left of the peak imply two episodes of growth. Initially, decay was rapid. The curve is truncated on the right side.

If we count an end point, the rain flux curve (Fig. 3b) shows three peaks. The primary peak leads the cloud-area peak by 3 to 4 h. Some rain falls before the first cold cloud appears.

As for flux, the flashes curve has a secondary peak after the main peak (Fig. 3b) and some flashes occur in the interval before the first cold cloud appears. Like the all-flashes curve, the positive-flashes curve also shows a secondary peak after the main peak. Unexpectedly (Rust et al, 1981; Stolzenberg, 1990), the main peaks in the flashes curves coincide; however, the positive-flashes second peak (at interval 10) does lag the flashes second peak. In the present case positive flash counts appear to offer little unique information on rain flux; hereafter, all comments on lightning refer to the total of positive and negative cloud-to-ground flashes.

The area curve is significantly smoother than either the flux or the flashes curves. It lags the other two by 3 to 4 h. Thus, flashes and flux are much better matched with each other than either is with area.

As might be expected from the profiles, scatter is large for area versus flux (Fig. 4) and area versus flashes (Fig. 5). It is small for flashes versus flux (Fig. 6). As a measure of the scatter in these plots, we calculated linear correlation coefficients for each pair of variables. These are shown at the top of Table 1, left side. Effectively, for the domain, area and flashes are unrelated. Area and flux are weakly related and flashes and flux are strongly related.

b. Large Domain

This part of the analysis is keyed to clouds. First, we present results for overlapping clouds; then, for storm systems; finally, for composited storm systems.

i. Overlapping Clouds

The set of all outlines for overlapping clouds (which includes storm systems as a subset of overlapping clouds) is shown in Fig. 7. All outlines lie in the south sector of the radar. Many lie partly or wholly beyond the 200 km range circle. Overlap is extensive. This overlap is in part a consequence of regeneration of storms and in part a consequence of repeated sampling of individual storms.

Rain flux in overlapping clouds tends to increase as cloud area increases (Fig. 8); it diminishes to zero as area goes to zero. However, some clouds produce no rain and overall the scatter is large. Compared with flux, there is a greater dispersion of points at low flash counts (Fig. 9). Scatter is greater for area versus flashes than for area versus flux. Flux versus flashes points cluster near the origin (Fig. 10). Small fluxes often occur in the absence of lightning.

For each of the three pairs there is less scatter in the overlapping cloud comparisons than in the small domain comparisons. This result is underscored by calculations of correlation coefficients, which are recorded in Table 1.

ii. Storm Systems

Storm systems are fairly well dispersed across and just outside of the large domain (Fig. 11). Movement is variable, especially from one storm system to another. Growth curves for the family of storm systems are shown in Fig. 12. In this figure the separation of any two paired points for a given storm system is proportional to the square root of the area of the system (an equivalent radius). We see not only a large range in sizes, but staggered growth of new storm systems as well. Except for one (number 6), we do not capture more than fragments of the larger storm systems. There is a great range of sizes and lifetimes; nevertheless, the area envelopes are smooth. Lifetime is positively correlated with size.

A comparison of curves in Fig. 12 shows that flashes peak well before area. Owing to more stringent limits on coverage, flux (Fig. 13) is more fragmented than area. Like flashes , it appears to peak before area.

Treating area in storm systems rather than in overlapping clouds has little effect on the scatter between area and flux (Fig. 14); still there are clouds with no rain. Neither is there much effect on the scatter between area and flashes (Fig. 15). Again we see clouds with no flashes. However, scatter between flux and flashes (Fig. 17) is reduced.

For the five storm systems (1, 2, 3, 5 and 6) which were fully or nearly fully covered by the Nashville radar, we accumulated area, flashes and rain flux. Plotting cumulative area and cumulative flashes as functions of rain flux yielded the distribution of points shown in Fig. 17. The sample is too small and highly skewed to support firm conclusions. Nevertheless (as we might expect from the work of Doneaud et al. (1981, 1984) and Atlas et al. (1990)), it indicates that the correspondence of cloud area and rain flux is very much stronger over the lifetime

of a system than at any stage of a system. Indeed, for this particular sample the gain from integration is sufficient to close the gap between area-flux correspondence and flash-flux correspondence.

iii. Composite Storm System

The composite is referenced to peak cloud area. It is based on the same storm systems which comprised the cumulative set. Of the five, one (number 6) is dominant. The first point of the area series for every storm system is assumed to be zero; however, the last point is "free" (i.e., not fixed at zero). Values are plotted at uniform intervals, each 1/9 of a storm system's period of existence. Interval 5 is forced to correspond to the peak of cloud area.

Apart from the double peak in Fig. 18a, the area curve is reasonably well-behaved (the double peak is a consequence of sampling). Flashes and flux both have single peaks (Figs. 18b and -c). Both peaks correspond with the first area peak. Thus (if we ignore the double peaking in the area curve) both flashes and flux peak about 2/9 of a cycle earlier than area. This is consistent with the phasing implied by the domain curves.

2. Threshold 226K

We expected fewer clouds at threshold 226K than at threshold 235K; also, smaller and more transient clouds. Otherwise, we expected areas calculated with the 226K threshold to correspond more closely with flash counts than those calculated with the 235K threshold. The results brought one or two surprises.

At threshold 226K over the small domain the area curve (Fig. 3a) was similar to that for 235K. The main difference was in their phases. Compared with threshold 235K, 226K area peaked about 2 h earlier.

Within the large domain the lower threshold temperature produced a slight improvement in the correspondence of overlapping cloud area to flux (Fig. 19; compare with Fig. 8; also see Table 1). Somewhat surprisingly, the the lower threshold temperature produced a deterioration (though small) in the correspondence between area and flashes. This is shown in the scatterplot (Fig. 20; compare with Fig. 9). The correlation of area to flashes dropped from 0.66 to 0.56 (Table 1).

The tracking process yielded seven storm systems. These are diagrammed in Fig. 21; their tracks are shown in Fig. 22. In general the threshold 226K storm systems are smaller and briefer than the 235K storm systems; however, in view of the deteriorations found for overlapping clouds the differences are slight. Movements are steadier than those of the threshold 235K storm systems; they tend to be directed toward the southeast.

Somewhat surprisingly, area for the threshold 226K storm systems appears to be about as well related to flux as it is for threshold 235K. This is shown in Fig. 23, which should be compared with Fig. 14 (also see Table 1). As for threshold 235K, area is not quite as well related to flashes as it is to flux (Figs. 24 and 15; also see Table 1).

E. DISCUSSION

In certain respects this study is severely limited. It employs a single technique for estimating rain from satellite images and a single radar for "measuring" rain. In addition, it treats a single outbreak of convection and less than a dozen rain systems. What makes the study unique is its simultaneous observation of cloud, rain and lightning in storms which are objectively identified and tracked.

Hitherto, the Williams and Houze (1987) algorithm has been applied to cloud clusters in the equatorial western Pacific. Evidently it identifies and isolates summertime thunderstorms and thunderstorm systems of the southeast United States as well. In its McIDAS incarnation the algorithm serves as an effective replacement for human judgement.

For an area which slightly exceeds the area of the largest convective system in our sample, we find that the fraction covered by cold cloud is poorly related to rain flux. In our case cold cloud within the small domain (75,000 km^2) explained less than 5% of the variance in rain flux within the small domain. The strength of the relationship appears to be less than that found by Richards and Arkin (1981) for rain systems of the eastern tropical North Atlantic Ocean, but consistent with that found by Negri and Adler (1987a) for rain systems over south Florida.

The poor relationship of area and flux can be attributed in part to a combination of two factors. First, it is the exception rather than the rule for rain to be uniform from front to back in the 13 July systems. Second, at times the radar observes only the fronts or only the backs of rain systems. The net effect of these two factors (also see Negri and Adler 1987a) is to diminish the representativeness of the radar's observations of the family of rain systems.

The relationship of cloud area to rain flux is much stronger if area is referred to individual cold clouds. Then area accounts for 65% to 70% of the variance in flux. This range encompasses the values found by Negri and Adler (1987b) in the "cloud definition" part of their south Florida study. It may fall just short of the highest value found by Richards and Arkin (1981) for 3 h averages over a 2.5^{o} block of the tropical North Atlantic.

For the small domain, area is completely unrelated to flashes. This surprising result is in part a consequence of mismatched phases. In addition it is in part a consequence of factors like those responsible for the weakness of the link between area and flux; that is, gradients in flash density from front to rear in clouds and incomplete observations of some clouds.

For both overlapping clouds and storms the link between area and flashes was fairly strong. Flashes explained 30% to 40% of the variance in area. This result is consistent with the experience reported by Cherna et al. (1985) in their test of a bispectral technique for detecting thunderstorms in GOES image pairs. Profiles for our composite storm system indicate that significant additional variance could be explained if flashes for a storm system were lagged before being correlated with area. The lag may be due to the mechanism which produces negative cloud-to-ground flashes. Field and laboratory observations indicate that this mechanism requires a strong updraft in a convective cell (e.g., see Lhermitte and Williams 1983, Goodman et al. 1988 and Williams 1989). Taking account of the work of

Sikdar et al. (1970) and Lo et al. (1982), this condition implies a correspondence of flashes to the expansion of the anvil of the cell rather than the area of the anvil.

The relationship of cumulative area to cumulative flux which we found through objective tracking is consistent with the very strong relationship which Smith et al. (1990) found through subjective tracking. However, owing to truncated observations we were able to treat only half of the storm systems which our objective approach identified. Furthermore, apart from the small-domain analysis, we did not attempt to assess the amount of rain missed by the temperature thresholding which underlies the tracking algorithm.

Our results conform with the idea that data on lightning can help to locate deep convective cores in GOES infrared images (e.g., see Davis et al., 1983; Goodman et al., 1988; and Christian, et al., 1989). They suggest as well that data on lightning can help to monitor the release of rain within a storm. They are consistent with the possibility that lightning data can help to scale the intensity of rain at a given location and time (see Goodman et al. (1988) and the papers referenced therein).

Information on location or timing or intensity in turn raises the question of how data on lightning could be worked into a rainfall algorithm. Suppose the issue is estimation of daily tropical rainfall and we have at our disposal (1) observations of cloud and lightning from an operational geostationary satellite, (2) access to registered, gridded coincident infrared images and flash counts. The simplest fused algorithm we can imagine thresholds the infrared image, estimates grid rain by a pixel version of GPI, counts flashes by grid box and adjusts the GPI estimate according to this count.

A variation of this scheme is suggested in part by our analysis of storm systems. In this variation we track cold clouds instead of counting cold grid pixels; estimate rain in proportion to cloud area and area change; count flashes by cloud; and then adjust the estimates according to the counts. The main advantage of this variation is higher resolution (at no cost in accuracy) in time and space.

The most radical variation of a fused scheme would be to start with the lightning data.

F. CONCLUSIONS

We have tested the proposition that lightning flash counts can improve satellite infrared estimates of rainfall. The test involves an outbreak of showers and thunderstorms over Tennessee and Alabama in July of 1986. Simultaneously this outbreak was observed by radar, GOES and the NASA Marshall lightning network. Cold-cloud area, flashes and rainfall were measured for a fixed area. They also were measured for storm systems, which are persisting cold clouds defined by a slightly modified version of the tracking algorithm of Williams and Houze (1987).

We found, first, that the "binary overlap" scheme of Williams and Houze was effective in isolating rain systems over the southeast United States. Second, whereas in the fixed area cold cloud fraction had no association with flash count, binary overlap rain systems were associated with high flash counts. Third, in such rain systems cloud area lagged both volume rain flux and flash count. Fourth, the associations are insensitive to threshold temperatures in the range 226K to 235K.

Finally, flash counts would improve GOES infrared rain estimates by reducing the uncertainty in rain area and in rain timing.

The study leaves several questions hanging--for example, Would the results change significantly for a threshold of, say, 244K? Are they representative of summertime thunderstorms of the South? Do the associations of area, flashes and flux depend on the scale of storm systems? Is the integral relationship indicated in Fig. 18 a fluke? Just how large a benefit should we expect from the addition of flash counts to infrared images? And would the same benefit accrue in the case of a technique which goes beyond mere cold cloud area?

APPENDIX A
Definitions

Binary image--two levels only, with the higher one corresponding to temperatures at or colder than some threshold.
Cloud (CL)--In a foreground image, an isolated cold spot. Each member of a pair of "coupled" cold spots is considered to be an individual cloud so long as the shared boundary is not more than 1/4 of the length of either unshared boundary; otherwise the pair is treated as a single cloud.
Overlapping cloud (OC)--In a foreground image, one or more clouds which intersect with a cloud or clouds in the background image.
Storm (ST)--an OC which (a) totals 4 or more (4 km by 8 km) pixels, (b) has an overlap area which either is half or more of the foreground CL area or half or more of the background CL area.
Storm system (SS)--Those ST's, OC's and CL's which proximity (in the case of clouds) or overlap in area bind into a sequence. "Proximity" is defined to include closeness (in location) from one image to the next; the proximity required of a cloud depends in part on the interval between images.

APPENDIX B
Conversion of Cloud Area to Volume Rain Flux

The technique called GOES Precipitation Index (see Arkin and Meisner 1987) assigns a rain rate of 3 mm/h to each cold pixel in an infrared image belonging to an hourly sequence. The areas of our clouds are given in (km^2). The units of volume rain flux are (10^2 kg/s) or (10^5 kg/s). Therefore, to convert cloud area to volume rain flux, multiply area by the factor 8.33 or 8.33*10^(-3).

REFERENCES

Adler, R.F., and R. A . Mack, 1984: Thunderstorm cloud height-rainfall rate relations for use with satellite rainfall estimation techniques. *J. Clim. Appl. Meteor.*, 23, 280-296.

Adler. R.F., and A. J. Negri, 1988: A satellite infrared technique to estimate tropical convective and stratiform rainfall. *J. Appl. Meteor.*,27, 30-51.

Arkin, P.A., and B.N. Meisner, 1987: The relationship between large-scale convective rainfall and cold cloud over the Western Hemisphere during 1982-84. *Mon. Wea. Rev.*,115, 51-74.

Atlas, D. and O. Thiele, eds., 1981: *Precipitation Measurements from Space.* Workshop Report, Goddard Space Flight Center, Greenbelt, MD, 358pp.

Battan, L.J., 1965: Some factors governing precipitation and lightning from convective clouds. *J. Atmos. Sci.*, 22, 79-85.

Beltrando, G., and D.L. Cadet, 1990: Interannual variability of the short rain season in East Africa: Relationships with general atmospheric circulation. *Veille Climatique Satellitaire*, Bulletin No. 33, ORSTOM, B.P. 147, Lannion 22302, France, 19-36.

Cherna, E., A. Bellon, G.L. Austin and A. Kilambi, 1985: An objective technique for the delineation and extrapolation of thunderstorms from GOES satellite data. *J. Geophys. Res.*, 90, 6203-6210.

Christian, H.J., R.J. Blakeslee and S.J. Goodman, 1989: The detection of lightning from geostationary orbit. *J. Geophys. Res. (Special Issue)*, 94, 13329-13337.

Davis, M.H., M. Brook, H. J. Christian, B.G. Heikes, R.E. Orville, C.G. Park, R.E. Roble and B. Vonnegut, 1983: Some scientific objectives of a satellite-borne lightning mapper. *Bull. Amer. Meteor. Soc.*, 64, 114-119.

Dodge, J., J. Arnold, G. Wilson, J. Evans and T. Fujita, 1986: The Cooperative Huntsville Meteorological Experiment (COHMEX). *Bull. Amer. Meteor. Soc.*, 67, 417-419.

Doneaud, A.A. and S. Ionescu-Niscov, D.L. Prignitz and D.L. Smith, 1984: The area-time integral as an indicator for convective rain volumes. *J. Clim. Appl. Meteor.*, 23, 555-561.

Doneaud, A.A., P.L. Smith, A.S. Dennis and S. Sengupta, 1981: A simple method for estimating the convective rain volume over an area. *Water Resources Res.*, 17, 1676-1682.

D'Souza, G., and E.C. Barrett, 1988: *A Comparative Study of Candidate Techniques for U.S. Heavy Rainfall Monitoring Operations Using Meteorological Satellite Data.* Final Report to the U.S. Dept. of Commerce, Dept. Geography, Univ. Bristol, UK, 39pp.

Goodman, S.J., D.E. Bueckler and P.J. Meyer, 1988: Convective tendency images derived from a combination of lightning and satellite data. *Weather and Forecasting*, 3, 173-188.

Goodman, S.J., D.E. Bueckler, P.D. Wright and W.D. Rust, 1988: Lightning and precipitation history of a microburst-producing storm. *Geophys. Res. Lett.*, **15**, 1185-1188.

Goodman, S.J., and H.J. Christian, 1992: Lightning. To appear as a chapter in *Global Change Atlas* (R. Gurney, J. Foster and C. Parkinson, eds.), Cambridge Univ. Press, New York.

Goodman, S.J., and D.R. MacGorman, 1986: Cloud-to-ground lightning activity in mesoscale convective complexes. *Mon. Wea. Rev.*, **114**, 2320-2328.

Griffith, C.G., W.L. Woodley, P.G. Grube, D.W. Martin, J. Stout and D.N. Sikdar, 1978: Rain estimation from geosynchronous satellite imagery: Visible and infrared studies. *Mon. Wea. Rev.*, **106**, 1153-1171.

Grosh, R., 1978: Lightning and precipitation -- the life history of isolated thunderstorms. *Preprints, Conf. on Cloud Physics and Atmospheric Electricity*, Issaquah, WA, Amer. Meteor. Soc., 617-624.

Haque, M.A., and M. Lal, 1991: Diagnosis of satellite-derived outgoing long wave radiation in relation to rainfall in India *Meteorol. Atmos. Phys.***45**, 1-13.

Heymsfield, G.M., and R. Fulton, 1988: Comparison of high-altitude remote aircraft measurements with the radar structure of an Oklahoma thunderstorm: Implications for precipitation measurement from space. *Mon. Wea. Rev.*,**116**, 1157-1174.

Joss, J., and A. Waldvogel, 1990: Precipitation measurement and hydrology. *Radar in Meteorology*, D. Atlas ed., Amer. Meteor. Soc., Boston, MA, 577-597.

Krider, E.P., R.C. Noggle, A.E. Pifer and D.L. Vance, 1980: Lightning direction-finding systems for forest fire detection. *Bull. Amer. Meteor. Soc.*, **61**, 980-986.

Lhermitte, R., and E. Williams, 1983: Cloud electrification. *Rev. Geophys. Space Phys.*, **21**, 984-992.

Lo, C.S., W.R. Barchet and D.W. Martin, 1982: Vertical mass transport in cumulonumbus clouds on day 261 of GATE. *Mon. Wea. Rev.*, **110**, 1994-2004.

Lyons, W.A., K.G. Bauer, A.C. Eustis, D.A. Moon, N.J. Petit and J.A. Schuh, 1989: R:SCAN's national lightning detection network: The first year progress report. *Preprints, Fifth International Conf. on Interactive Information and Processing Systems for Meteorology, Oceanography and Hydrology.* Anaheim, CA, Amer. Meteor. Soc., 29 Jan.--3 Feb. 1989, 241-248.

Martin, D.W., and A.J. Schreiner, 1981: Characteristics of West African and east Atlantic cloud clusters: A survey from GATE. *Mon. Wea. Rev.*, **109**, 1671-1688.

McAnelly, R.L., and W.R. Cotton, 1989: The precipitation life cycle of mesoscale convective complexes over the central United States. *Mon. Wea. Rev.*, **117**, 784-808.

Negri, A.J., and R.F. Adler, 1981: Relation of satellite-based thunderstorm intensity to radar-estimated rainfall. *J. Appl. Meteor.*, **20**, 288-300.

Negri, A.J. and R.F. Adler, 1987: Infrared and visible satellite rain estimation. Part I: A grid cell approach. *J. Clim. Appl. Meteor.*, **26**, 1553-1564.

Negri, A.J. and R.F. Adler, 1987: Infrared and visible satellite rain estimation. Part II: A cloud definition approach. *J. Clim. Appl. Meteor.*, **26**, 1565-1576.

Orville, R.E., R.W. Henderson and L.F. Bosart, 1983: An east coast lightning detection network. *Bull. Amer. Meteor. Soc.*, **64**, 1029-1037.

Orville, R.E., and D.W. Spencer, 1979: Global lightning flash frequency. *Mon. Wea. Rev.*, **107**, 934-943.

Raymond, D.J., and A.M. Blyth, 1989: Precipitation development in a New Mexico thunderstorm. *Quart. J. Royal Meteor. Soc.*, **115**, 1397-1423.

Richards, F., and P. Arkin, 1981: On the relationship between satellite-observed cloud cover and precipitation. *Mon. Wea. Rev.*, **109**, 1081-1093.

Rosenfeld, D., D. Atlas and D.A. Short, 1990: The estimation of convective rainfall by area integrals. Part II: The Height-Area Rainfall Threshold (HART) method. *J. Geophys. Res.*, **95**, 2161-2176.

Sikdar, D.N., V.E. Suomi and C.E. Anderson, 1970: Convective transport of mass and energy in severe storms over the United States -- an estimate from a geostationary altitude. *Tellus*, **22**, 521-532.

Williams, E.R., 1989: The tripole structure of thunderstorms. *J. Geophys. Res.*, **94**, 13151-13167.

Williams, E.R., M.E. Weber and R.E. Orville, 1989: The relationship between lightning type and convective state of thunderclouds. *J. Geophys. Res.*, **94**, 13213-13320.

Williams, M. and R.A. Houze, Jr., 1987: Satellite-observed characteristics of winter monsoon cloud clusters. *Mon. Wea. Rev.*, **115**, 505-519.

Williams, S.F., H.M. Goodman, K.R. Knupp and J.E. Arnold, 1987: Space/COHMEX Data Inventory Document. *NASA Tech. Memo 4006*, Scientific and Technical Information Office, Code NTT-4, Washington, D.C. 20546-0001, 480pp.

Table 1. Linear regression coefficients of correlation (right of diagonal) and sample size (left of diagonal) for cloud area, volume rain flux and total flashes. Part (a), small domain; part (b), large domain overlapping clouds; part (c), large domain storm systems.

Domain		Threshold 235K			Threshold 226K		
		area	flux	flashes	area	flux	flashes
a.	area	--	0.15	-0.04	--	0.15	-0.02
	flux	11	--	0.88	11	--	0.88
	flashes	11	11	--	11	11	--
b.	area	--	0.83	0.66	--	0.86	0.56
	flux	30	--	0.96	18	--	0.95
	flashes	47	30	--	32	18	--
c.	area	--	0.82	0.63	--	0.84	0.53
	flux	17	--	0.95	13	--	0.95
	flashes	28	17	--	32	13	--

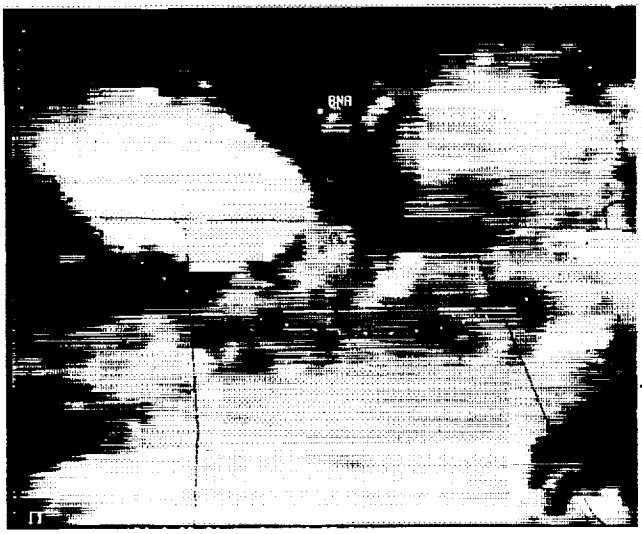

(a)

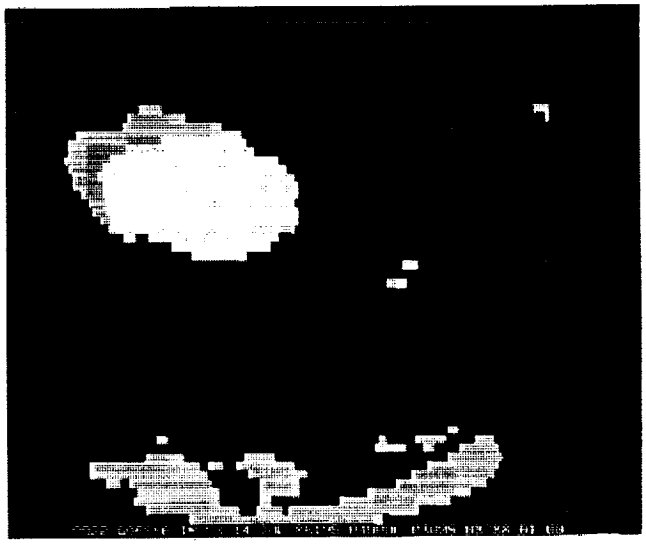

(d)

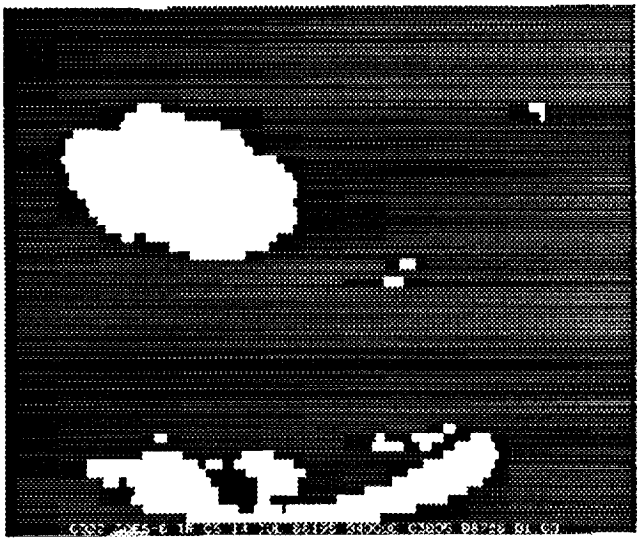

(b)

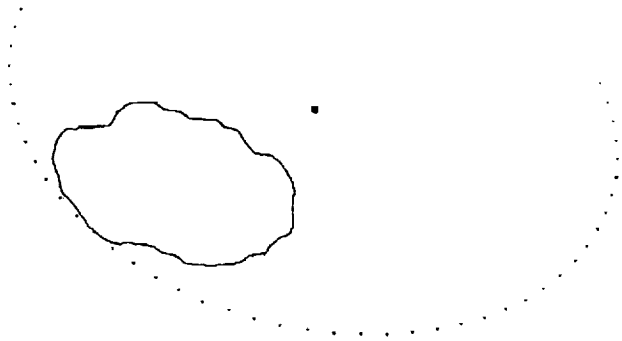

(e)

(c)

FIG. 1. Illustration of the binary overlap and cloud outlining procedure. (a) Sector of the 0400 UTC full resolution GOES infrared image for 14 July 1986. The sector is roughly centered on Huntsville, Alabama. State boundaries are overlaid. "BNA" marks the location of the Nashville, Tennessee, National Weather Service radar. Dotted arc around BNA marks the 240 km range circle. (b) Part (a) image with a binary enhancement. Pixels at and colder than 235K are white; warmer than 235K are black. (c) Sector of the 0500 UTC image for 14 July 1986; same area as (a). The part (b) binary enhancement has been applied. (d) Superposition of images in (b) and (c). Shading convention is as follows: warm/warm, black; (b) warm/(c) cold, dark grey; (b) cold/(c) warm, light grey; and cold/cold, white. (e) Outline of the largest overlapping cloud at 0400 UTC.

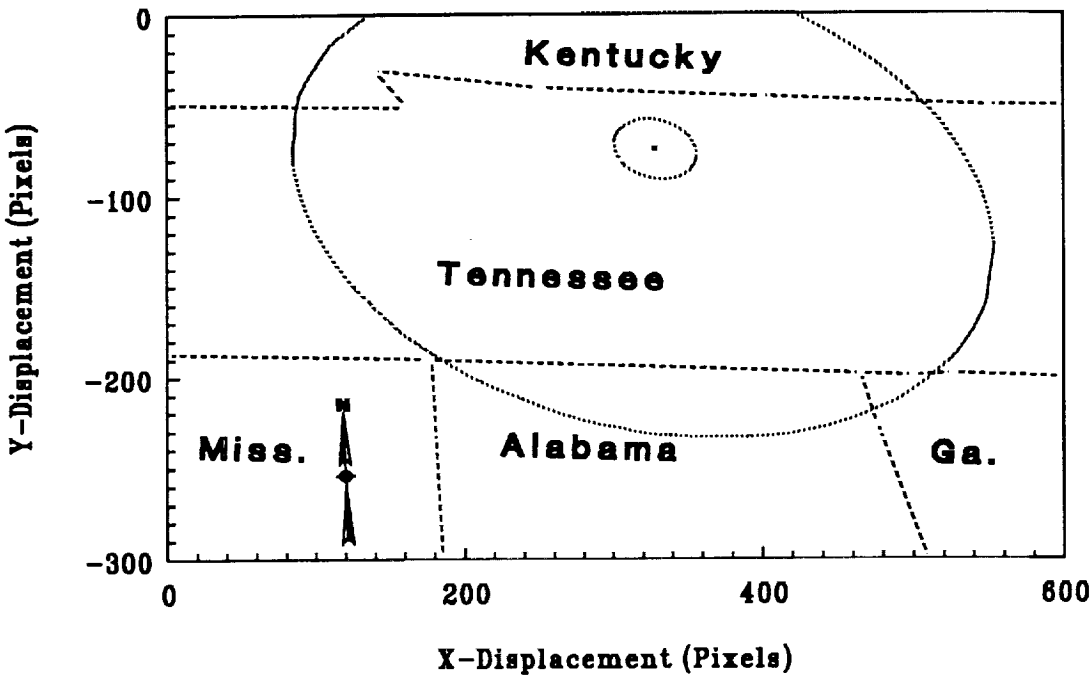

FIG. 2. Map of the small domain, with state boundaries.

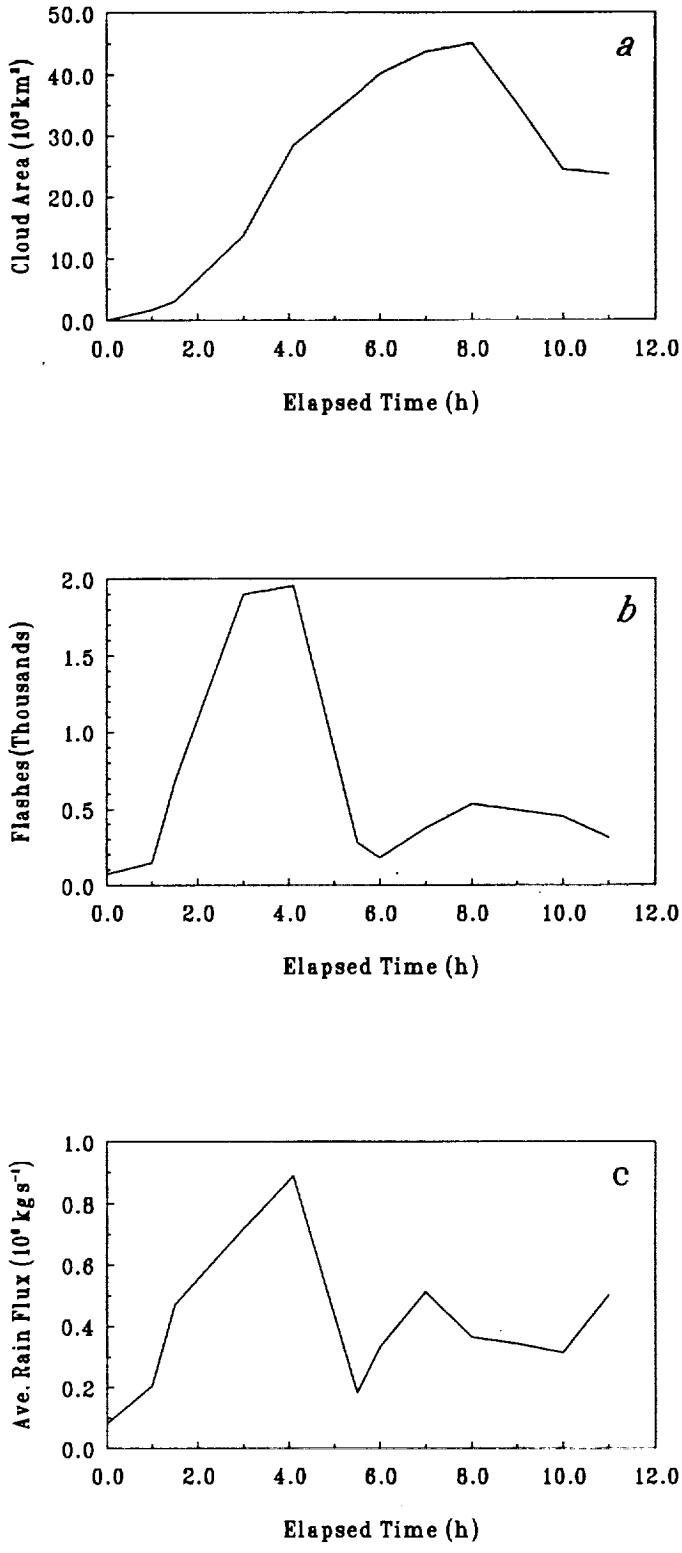

FIG. 3. Plots of small domain cloud area, rain flux and flash count as a function of time. The threshold for cloud area in this and following plots is 235K.

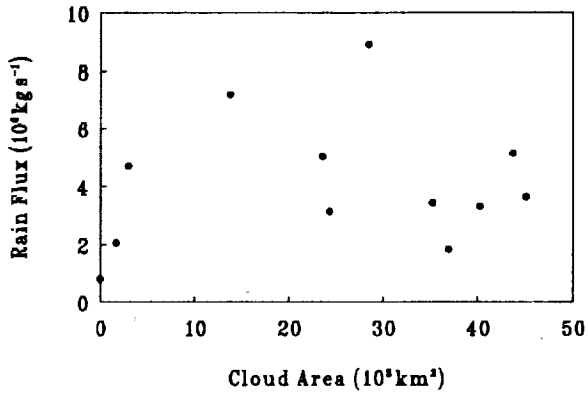

FIG. 4. Scatter plot of cloud area versus rain flux for the small domain.

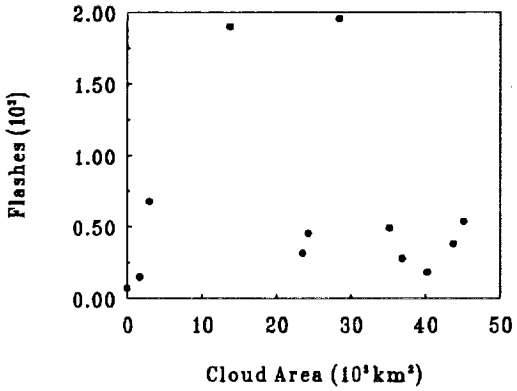

FIG. 5. Scatter plot of cloud area versus positive and negative flash count.

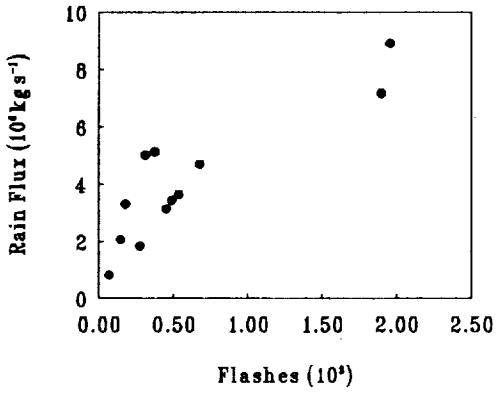

FIG. 6. Scatter plot of rain flux versus flash count.

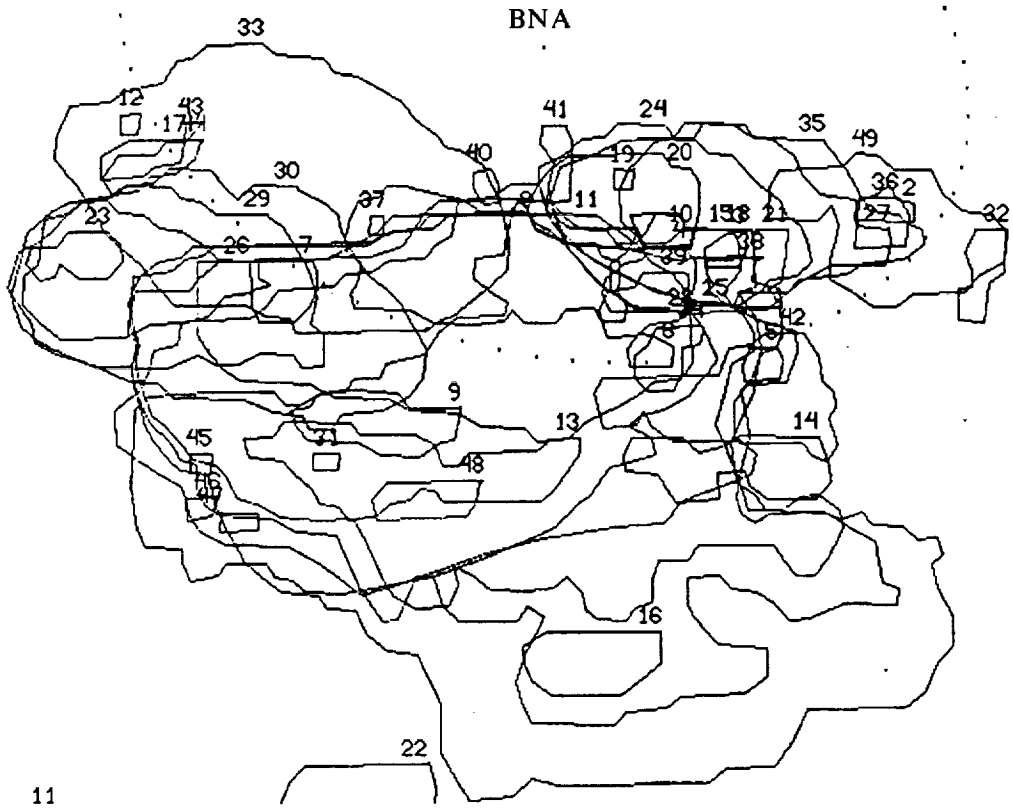

FIG. 7. Plot of all outlines and outline numbers. Also shown is the location of the Nashville radar and the 200 km range circle.

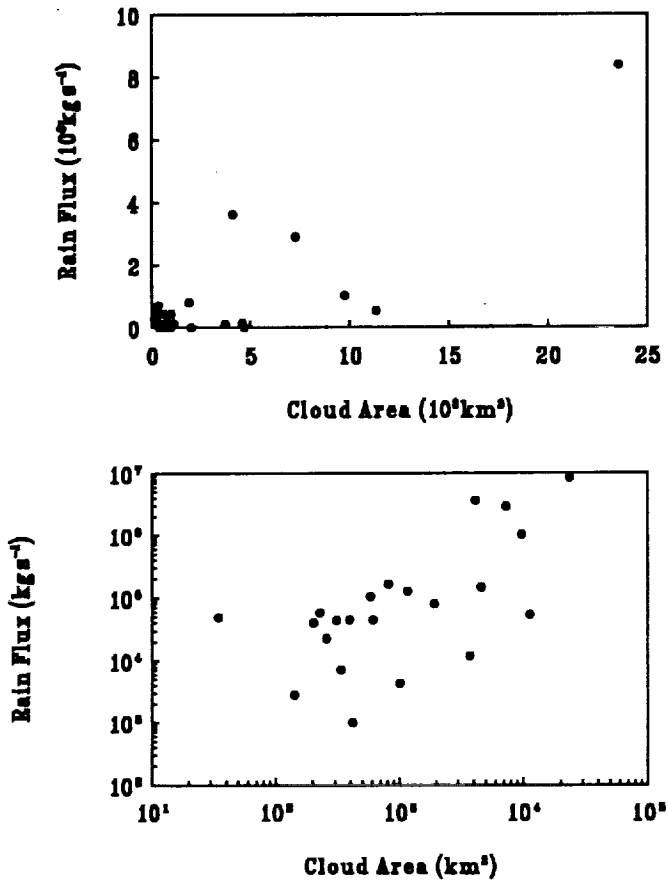

FIG. 8. Scatter plot of cloud area versus rain flux for overlapping clouds. Top panel shows all values; coordinates are linear. Bottom panel excludes zero rain-flux points; coordinates are logarithmic.

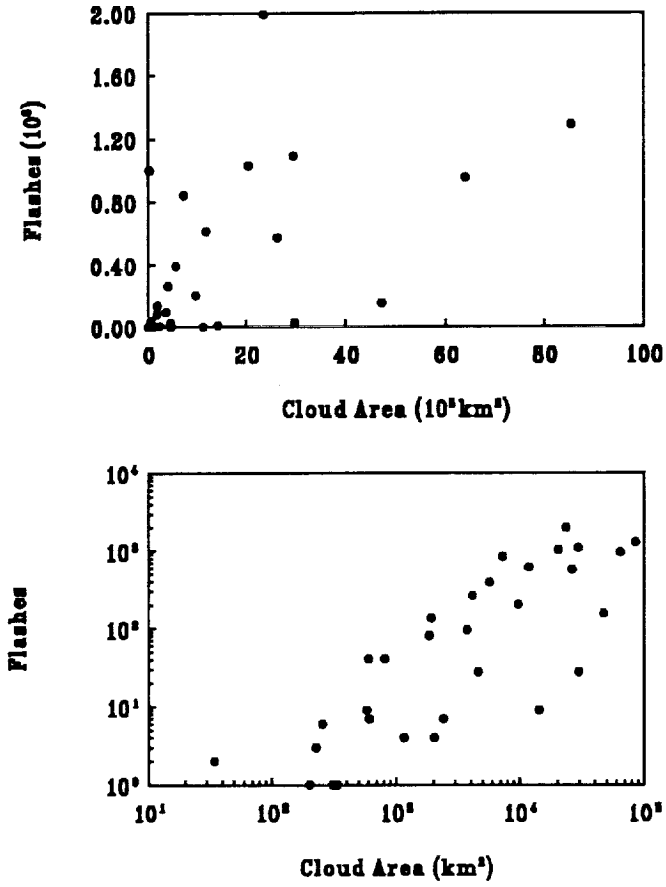

Fig. 9. As for Fig. 8, except cloud area versus flash count and bottom panel excludes zero flash-count points.

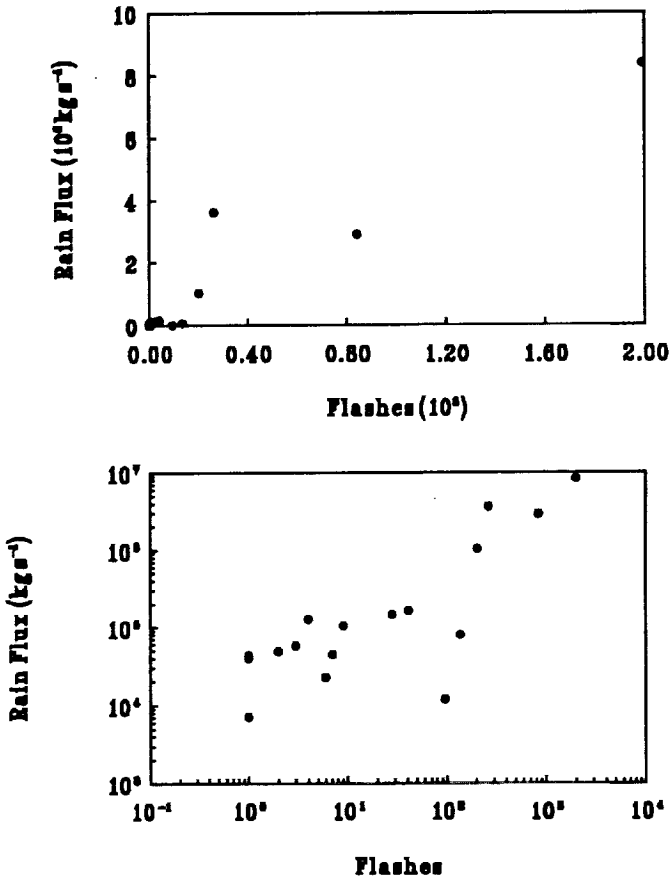

FIG. 10. As for Fig. 8, except rain flux versus flash count and bottom panel excludes all zero points.

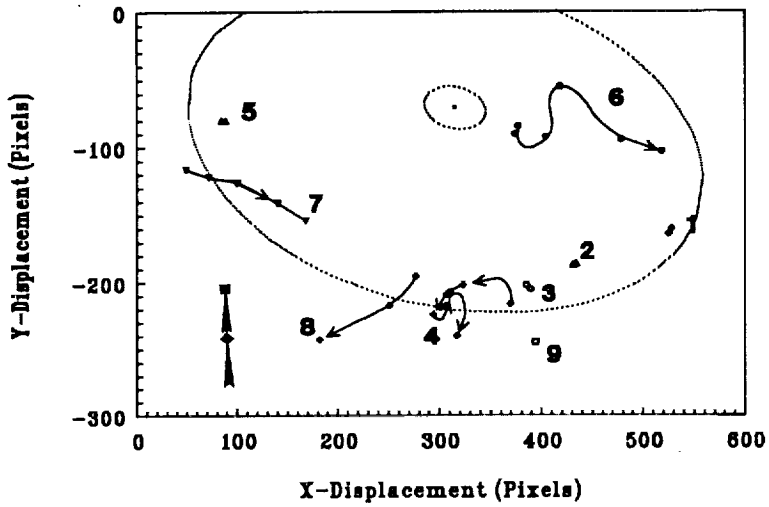

FIG. 11. Map of the locations of the centers of storm systems. Numbers differentiate storm systems; arrows indicate movement.

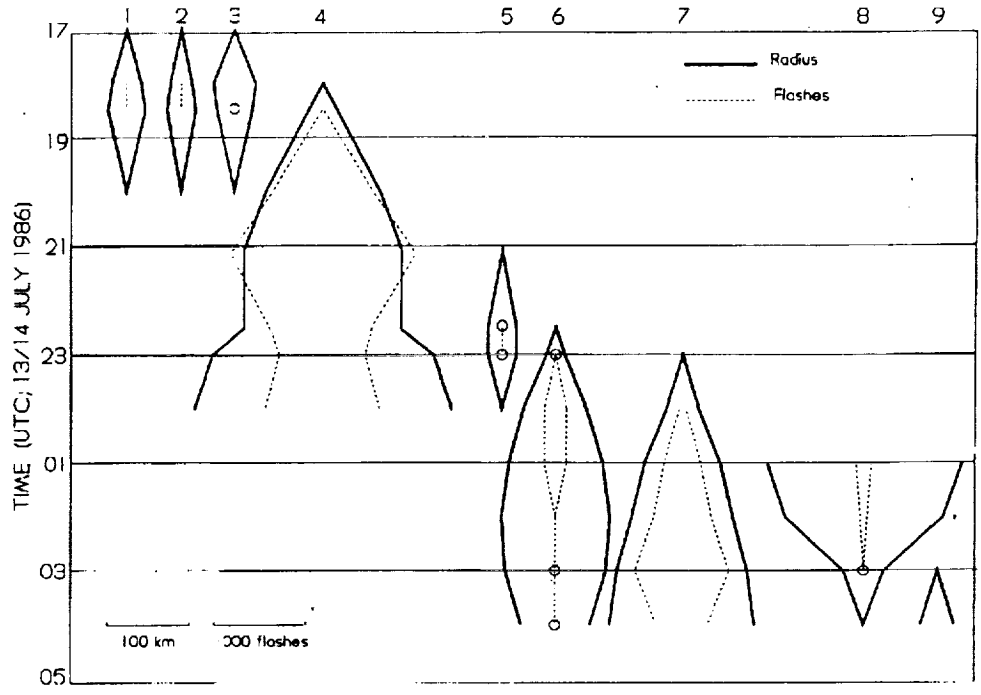

FIG. 12. Area and flash life-histories of storm systems. Numbers across the top of the figure correspond with the storm system numbers in Fig. 11. Solid lines symmetric about vertical (time) axes through each storm number represent storm equivalent radius. Dashed lines represent storm flash count. A zero count is indicated by a circle along the flash profile.

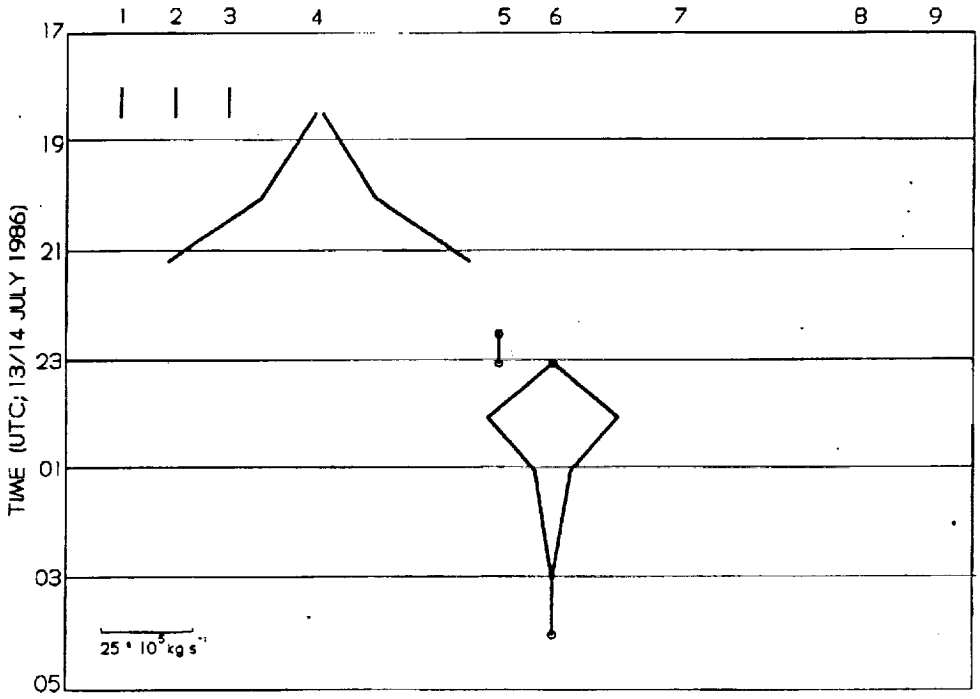

FIG. 13. As for Fig. 12, except rain flux.

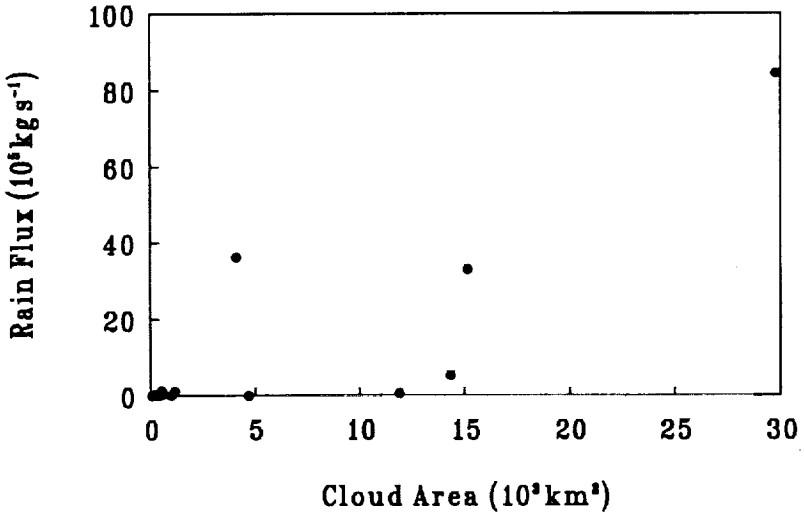

FIG. 14. Scatter plot of cloud area versus rain flux for storm systems.

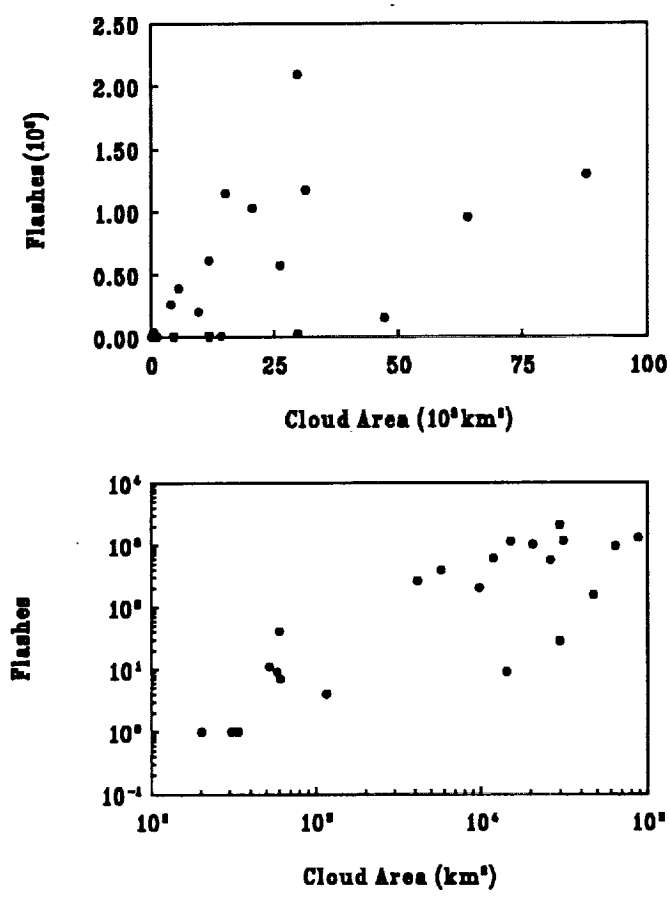

FIG. 15. Scatter plot of cloud area versus total flash count for storm systems. The top panel shows points in a linear coordinate system. The bottom panel excludes points having zero flash count and presents the remaining points in a logarithmic coordinate system.

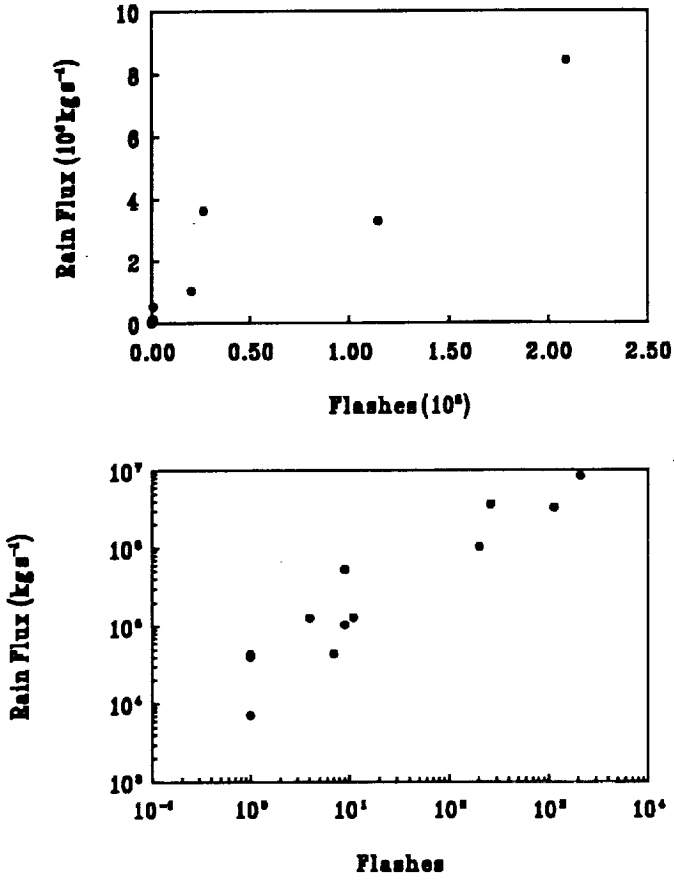

FIG. 16. As for Fig. 15, except rain flux versus total flash count. All zero points are excluded from the bottom panel.

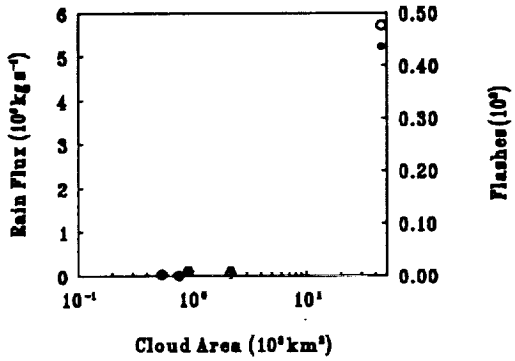

FIG. 17. Scatter plot of cloud area versus cumulative flash count (open circles) and cumulative rain flux (dots) for long-lived storm systems. Note that area is plotted on a logarithmic scale.

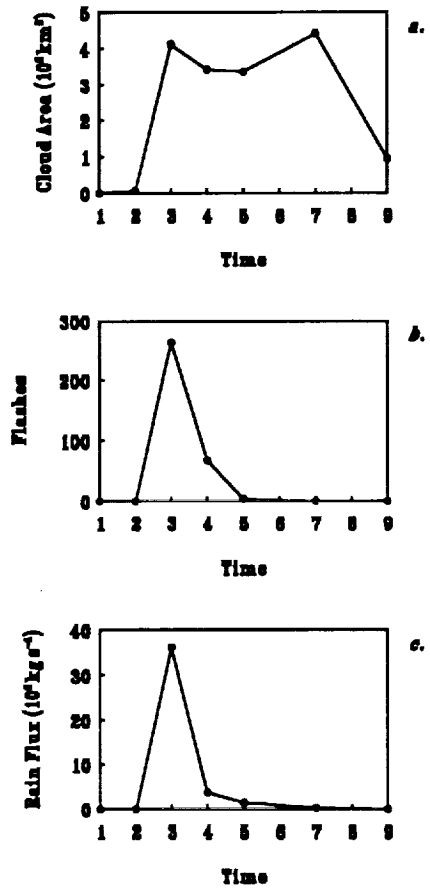

FIG. 18. Plot of cloud area, flash count and rain flux for the composite storm system. "Time" refers to the nine divisions which are defined for the composite storm system. In every case time 5 coincides with the time of the peak in storm system area and time 1 with the time of the last zero value before the storm appears. (a) Cloud area. (b) Flash count. (c) Rain flux.

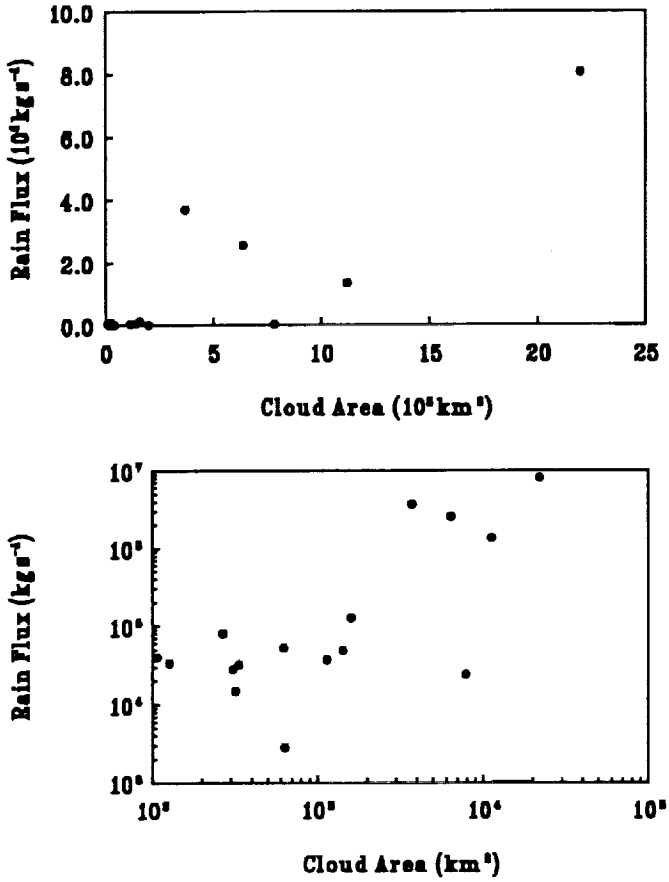

FIG. 19. Scatter plot of cloud area versus rain flux for overlapping clouds in the threshold 226K image series. Top panel shows points in a linear coordinate system; bottom panel excludes points of zero flux and plots remaining points in logarithmic coordinates.

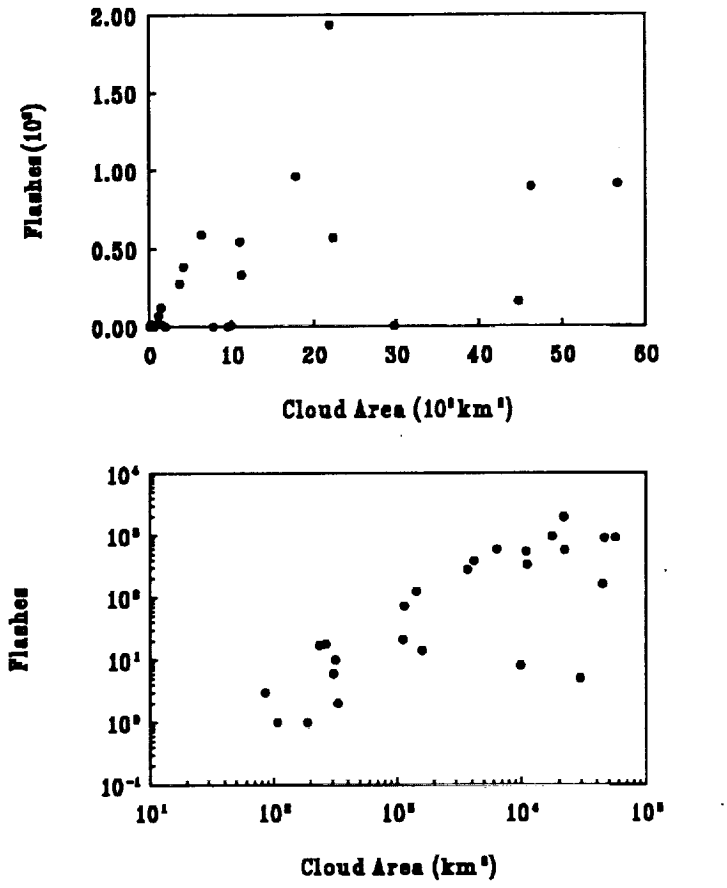

FIG. 20. As for Fig. 19, except cloud area versus flash count.

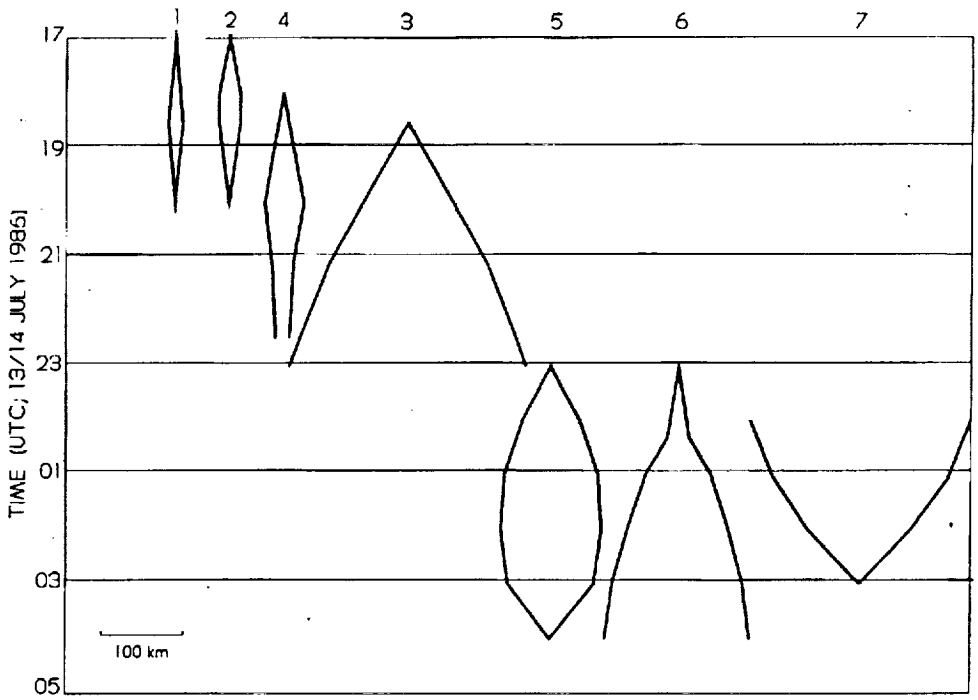

FIG. 21. Equivalent Radii of storm systems for a threshold of 226K. numbers across the top correspond with the storm system numbers in Fig. 22.

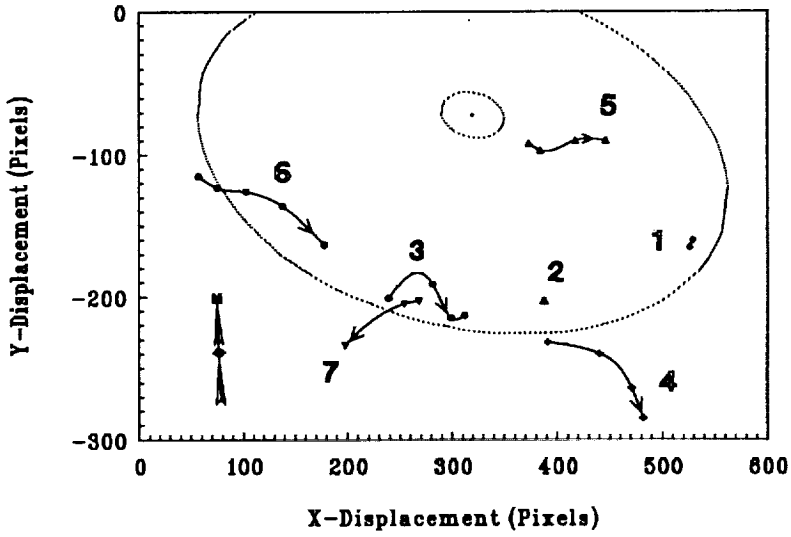

FIG. 22. Map of the locations of the centers of storm systems like Fig. 11, except threshold 226K. Numbers differentiate storm systems; arrows indicate movement.

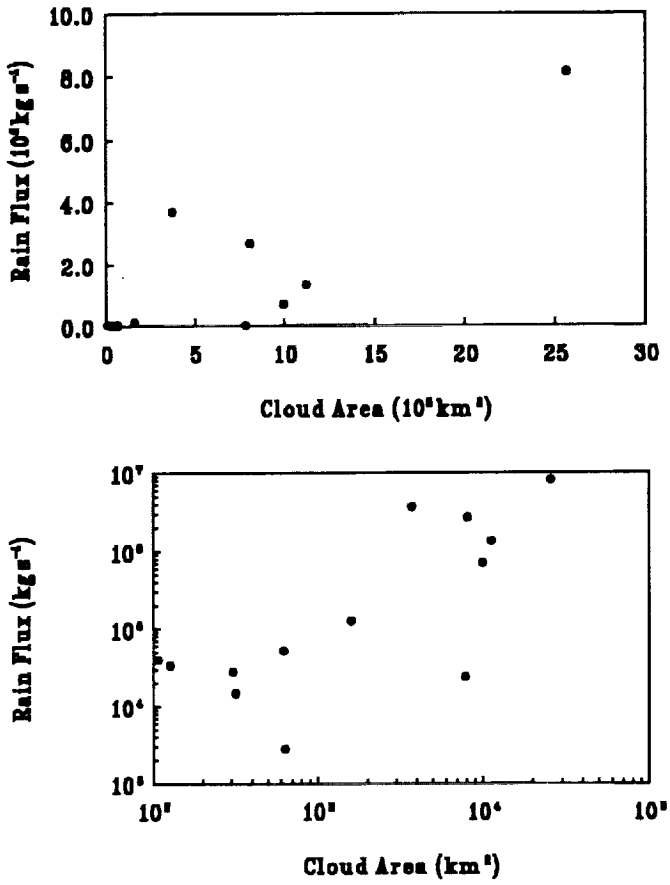

FIG. 23. Scatter plot of cloud area versus rain flux, threshold 226K. Otherwise, as for Fig. 15.

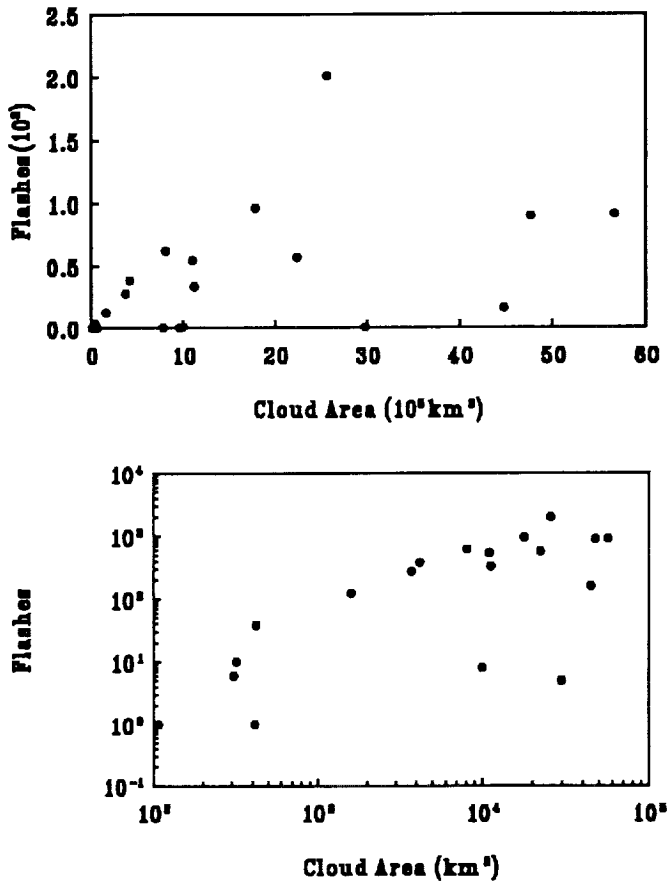

FIG. 24. As for Fig. 23, except cloud area versus total flash count.